Flux Density Waveform Reconstruction Method for Efficient Finite Element Analysis of Electric Motors



*Published Version:*
Capitanio, A., Sala, G., Nuzzo, S., Rizzoli, G., Barater, D., Franceschini, G. (2024). Flux Density Waveform Reconstruction Method for Efficient Finite Element Analysis of Electric Motors. IEEE [10.1109/icem60801.2024.10700552].

*Availability:*
This version is available at: https://hdl.handle.net/11585/995982 since: 2025-03-31

*Published:*

DOI: http://doi.org/10.1109/icem60801.2024.10700552

# Flux Density Waveform Reconstruction Method for Efficient Finite Element Analysis of Electric Motors

Alessandro Capitanio
*University of Modena and Reggio Emilia*
*DIEF*
Modena, Italy
alessandro.capitanio@unimore.it

Giacomo Sala
*University of Bologna*
*DEI*
Bologna, Italy
g.sala@unibo.it

Stefano Nuzzo
*University of Modena and Reggio Emilia*
*DIEF*
Modena, Italy
stefano.nuzzo@unimore.it

Gabriele Rizzoli
*University of Bologna*
*DEI*
Bologna, Italy
gabriele.rizzoli@unibo.it

Davide Barater
*University of Modena and Reggio Emilia*
*DIEF*
Modena, Italy
davide.barater@unimore.it

Giovanni Franceschini
*University of Modena and Reggio Emilia*
*DIEF*
Modena, Italy
giovanni.franceschini@unimore.it

***Abstract*—This paper proposes a procedure for optimizing the electromagnetic finite element analysis of synchronous electric motors. The methodology allows for the retrieval of the solution of the problem in an entire rotor rotation starting from simulations carried out within a reduced angle range, corresponding to the half of the electrical period divided by the number of phases of the motor winding. This is achieved by exploiting the geometrical periodicities of the motor and by dividing the static and rotating parts of the model in homologous sectors, which will undergo the exact same magnetic state, but with shifted waveforms with respect of the rotor angle. By properly rearranging the parts of the waveform taken from the different sectors, it is possible to reconstruct the full waveform in each part of the motor. A method to determine the waveform reconstruction sequence, i.e. the order in which the information should be taken from the different stator and rotor sectors, is defined as a function of the motor parameters. While a similar approach has been already presented in literature for specific motor designs and with the purpose of estimating iron losses, in this paper the methodology is generalized for motors with an arbitrary number of phases and is valid both for integer and fractional winding motors.**

***Index Terms*—Finite Element, Electromagnetic Simulation, Multi-phase, Waveform Reconstruction**

## I. Introduction

The design procedure of electric motors often relies upon finite element (FE) electromagnetic simulations, which allow to achieve accurate results and to take into account the non-linear magnetic properties of the ferromagnetic materials. However, even with modern computer hardware, electromagnetic FE simulations result computationally intensive and may eventually lead to several hours of simulation time, which means that the optimization of the simulation procedure is still very valuable. One of the solutions used to reduce the computation time is to simulate only a fraction of the motor geometry, exploiting the geometrical symmetries of the motor and imposing periodic or anti-periodic boundary conditions at the boundaries of the simulated portion, which is already widely implemented in most electromagnetic FE software packages, such as Altair Flux™ [1] or JMAG® [2]. In addition, the characterization of a motor requires to run multiple simulations at different rotor angle positions, in order to retrieve the waveforms of the main quantities of interest, such as torque or flux linked with the windings. Therefore, another very important aspect is to determine the minimum angle range to be simulated, as well as the number of rotor positions to simulate within this range, which will determine the waveform resolution. Regarding the angle range to be simulated, one of the possible approaches would be to set it equal to the period of the quantity to be retrieved. For example, if torque is the only parameter of interest, simulations could be run within the torque ripple period only, while if iron losses have to be calculated in post-processing, the angle range has to be set at least equal to the flux density waveform period, which is always higher. This approach however does not take into account the geometrical periodicities of the electromagnetic solution of the motor. In fact, if certain geometrical periodicity constraints, that will be specified in section II, are met, the motor geometry can be divided into homologous sectors that are geometrically equal and feature the same flux density distribution waveforms, but simply shifted in phase with respect to the rotor angle. This allows to reconstruct the overall waveform of any variable of the electromagnetic solution starting from an angle range corresponding to only half of the electrical period divided by the number of phases, as it will be demonstrated in section IV. The benefit given by this procedure is that the number of steps to be simulated with a given angular resolution can be reduced, or that the angular resolution can be increased for a given total number of simulated steps. A similar approach has already been implemented for determining iron losses from FE simulations in [3], specifically for a yokeless axial flux motor, and in [4], for a generic radial-flux synchronous generator. In [5], the geometrical periodicities has been similarly exploited, but for the purpose of reconstructing an approximate waveform from a single static simulation, instead of reducing the number of steps required by an angle stepping simulation with a given resolution. While the mentioned papers also hinted at possible applications of such approach for other motor topologies, in this paper the procedure is generalized for different motor layouts, both for integer and fractional slot windings, and for any number of phases. The generalization allows for the potential inclusion of the procedure in FE software packages, especially in cases where the motor geometry is derived from a template already available within the software.

## II. Motor Multiplicities

Synchronous electric motors with a number of pole pairs higher than one may feature geometrical symmetries that allow to retrieve the electromagnetic solution of the complete motor while actually solving one portion of its geometry. This is commonly exploited in FE software packages, which offer the possibility of simulating only a slice of the motor using periodic or anti-periodic boundary conditions, as explained in [6]. The fraction of the motor to be simulated is defined by the number of multiplicities (i.e. the number of times the motor geometry repeats itself angularly). For example, for slotted motors, the multiplicity $m$ is given by the greatest common denominator (GCD) between the number of stator slots per phase and the rotor pole number, as reported in (1).

$$m = \mathrm{GCD}\left(\frac{N_s}{n_{ph}}, 2p\right) \rightarrow \theta_s = \frac{2\pi}{m} \tag{1}$$

In (1), $N_s$ is the number of stator slots, $n_{ph}$ is the number of phases, $p$ is the number of pole pairs, and $\theta_s$ is the mechanical angle representing the portion of the motor to be simulated.
It can be noted that for winding configurations featuring an integer number of slots per-pole per-phase, $m$ will result equal to the number of poles $2p$, as $N_s/n_{ph}$ will be proportional to $2p$, meaning that a multiplicity will correspond to one pole pitch only. This will allow for significant simplification of the waveform reconstruction procedure for integer-slot windings, as it will be explained later.

## III. Geometrical Periodicity

Within the simulated motor portion, another level of geometrical periodicity is required to allow for the reconstruction of the flux density in both the stator and rotor regions.

The geometrical periodicities required are

- **for the stator**: the geometry should be periodical within the motor multiplicity a number of times equal to the number of phases. Therefore, the geometry should be composed by $n_{ph}$ equal sectors with an angular extension corresponding to $\theta_{ph}$: the angular extension of one motor multiplicity divided by the number of phases, (see (2)).

$$\theta_{ph} = \frac{2\pi}{m}\frac{1}{n_{ph}} \tag{2}$$

- **for the rotor**: the geometry should be periodical within the motor multiplicity a number of times equal to the number of poles present in a single multiplicity. Therefore, the geometry should be composed by $2p/m$ equal sectors with an angular extension corresponding to $\theta_p$: the angular extension of one motor pole (see (3)).

$$\theta_p = \frac{\pi}{p} \tag{3}$$

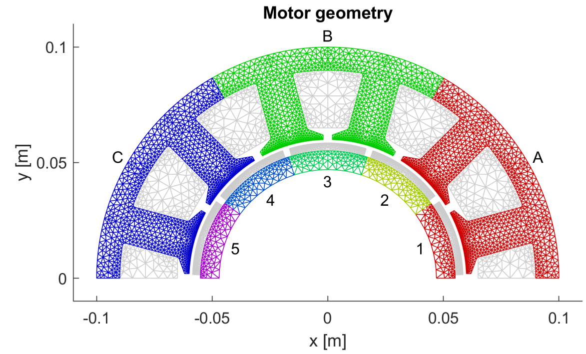

Fig. 1. 12 slot, 10 poles double layer concentrated winding motor.

These conditions are typically inherently met unless details due to non-electromagnetic requirements, such as stator lamination retention grooves or holes, are included in the geometry. It is also worth to remind that, for the practical implementation of the waveform reconstruction method described in this paper, the geometrical periodicities listed above must be guaranteed also at the mesh level. Moreover, since the mesh in the stator and rotor regions should not vary as the rotor rotates, the stator-rotor interface at the air gap should be implemented using techniques that avoids the re-meshing of the stator and rotor regions during rotation. For this purpose, both *sliding band* and *moving band* methods can be used [7] [8]. The suggested solution is to use the sliding band method while imposing a constant segment length at the air gap boundary, and, when possible, to set the rotor rotation angle step as a multiple of the angle corresponding to the boundary air gap mesh segment. In such way, the stator and the rotor mesh always snap coherently avoiding interpolation and thus minimizing numerical noise in the results.
Figure 1 shows the geometry of a generic 12 slots, 10 poles double-layer concentrated winding (DLCW) motor that will be used as an example in this paper. Colors identify the different stator and rotor yoke sectors. The following sector nomenclature and the reference frame are also introduced:

- the naming of the stator sectors is given by letters in alphabetical order assigned in anti-clockwise direction;
- the naming of the rotor sectors is given by integer numbers assigned in anti-clockwise direction;
- the mechanical rotation angle of the rotor is considered positive if anti-clockwise.

## IV. Flux Density Waveform Reconstruction

In this section, the periodicity of the flux density will be analyzed separately for the stator and rotor regions, with the purpose of determining the minimum angle range to be simulated. Then, a generalized method to determine the order and the polarity in which the information should be taken from the various sectors will be presented. Before proceeding, it is worth reminding that to ease the physical understanding of the approach the flux density is the only mentioned variable. Nevertheless, all of the assumptions are actually valid for any variable derived from the electromagnetic solution of the problem, which is defined by the magnetic vector potential, from which the magnetic field and the flux density itself are derived quantities.

### A. Reconstruction of stator waveform

The stator region undergoes magnetic flux density oscillations due to both the supplied current and the interaction with the rotating rotor. The first depends on the electrical frequency of the supply, the second on the rotor speed. Being the motors under study synchronous, both effects cause flux oscillations which are equally repeating in one electrical period of time. The waveform is also symmetric, and thus, is sufficient to obtain half of it to retrieve the complete one. Considering the geometrical periodicities listed in section II, it can be demonstrated that the flux density waveforms taken in its radial and tangential coordinates, in any point of a given stator sector, are equivalent to those of the homologous points found in the other sectors, which are at the same radial coordinates and spaced by the angular extension of a stator phase sector, $\theta_{ph}$. The waveforms, consequently, will also result shifted in phase by an angle corresponding to $\theta_{ph}$, but in opposite direction, as it can be appreciated in Fig. 2. Exploiting this aspect, the full waveform in any point of the stator geometry can be reconstructed performing simulations within an angle range $\theta_{sim}$ corresponding to half of the electrical period divided by the number of phases of the motor winding, as given in (4).

$$\theta_{sim} = \frac{\pi}{p}\frac{1}{n_{ph}} \tag{4}$$

The reconstruction sequence, i.e. the order in which the information should be taken from the various stator sectors and their respective polarity, can be determined in a generalized form as a function of the motor characteristics. In this paper, such sequence will be defined by a vector containing the $n_{ph}$ letters identifying the different stator sectors, with the minus sign used for indicating inverted polarity. Such sequence leads to the reconstruction of half of the waveform, while for the complete one, it is sufficient to repeat the sequence with inverted polarity due to the symmetry property previously mentioned. The reconstruction sequence will be presented only for the first stator sector, labeled "A" according to the adopted nomenclature. Once the waveform is reconstructed for one sector, it will be trivial to retrieve it for the remaining ones by applying the proper phase shift. The solution is presented both for the specific configurations which feature an integer number of slots per pole per phase, such as traditional distributed winding layouts, and in a generalized form, valid also for configurations with a fractional number of slots per pole per phase, such as the DLCW motor shown in Fig. 1.

For **integer-slot windings**, which according to (1) feature one pole per multiplicity, a sector shift is equivalent to a

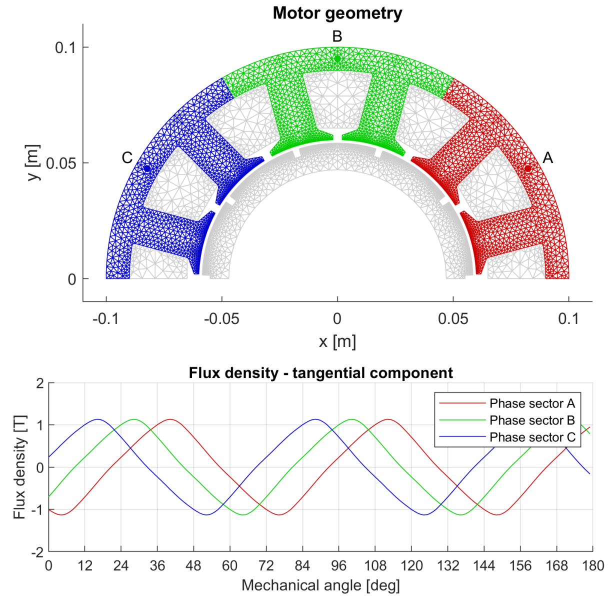


Fig. 2. Example of flux density waveforms in the three phase sectors of the stator. Waveforms refer to the points highlighted in the top figure. Motor supplied with Iq current only.

negative rotor rotation of $\theta_{sim}$, since in such case $\theta_{ph} = \theta_{sim}$. Therefore, according to the nomenclature specified in section II, the reconstruction sequence for section A proceeds in reversed alphabetic order and with inverted polarity. For example, the reconstruction sequence for the first stator sector of a six-phase motor with distributed winding would result as $[+\mathrm{A}, -\mathrm{F}, -\mathrm{E}, -\mathrm{D}, -\mathrm{C}, -\mathrm{B}]$.

For **fractional-slot windings**, which feature multiple poles per multiplicity, the phase shift angle corresponds to $2p/m$ times the simulation angle $\theta_{sim}$, which makes the definition of the reconstruction sequence less trivial. For such purpose, the following methodology is proposed.

First of all, the number of phase sector shifts $k_{ph}$ that leads to an equivalent waveform shift corresponding either to $\theta_{sim}$, or to $\theta_{sim} + \theta_p$ if with reversed polarity (since $\theta_p$ is half of the waveform period) is identified solving (5), where $k_p$ is an integer number.

$$-k_{ph}\theta_{ph} + k_p\theta_p = \theta_{sim} \tag{5}$$

Substituting in (5) $\theta_{ph}$, $\theta_p$, and $\theta_{sim}$ from (2), (3) and (4), equation (6) is obtained, where a dependency on the number of poles per multiplicity $2p/m$ and the number of phases $n_{ph}$ only is observed.

$$-k_{ph}\frac{2p}{m} + k_p n_{ph} = 1 \tag{6}$$

Equation (6) represents a linear Diophantine equation in the form: $ma + nb = \gcd(a, b)$ where $a = 2p/m$, $b = n_{ph}$, $m = -k_{ph}$, $n = k_p$, and $\gcd(a, b) = 1$ since $2p/m$ and $n_{ph}$ are inherently co-prime due to the multiplicity definition. Such problem, according to Bézout's identity, has a family of possible solutions and can be solved using the Euclidean algorithm [9]. The pair of coefficients to be taken from the family of solutions is the one that minimizes $k_{ph} = -m$ from the ones that have $m < 0$ and $n > 0$, since both $k_{ph}$ and $k_p$ must be positive integers. By a practical point of view, such solution can also be found by searching via a nested for cycle the only $k_{ph}$ and $k_p$ combination that satisfies eq. (6) with $1 \leq k_{ph} < n_{ph}$ and $1 \leq k_p < 2p/m$.

Once $k_{ph}$ is determined, the sequence in which the information should be taken from the $n_{ph}$ stator sectors can be retrieved. Starting from the known simulated part, the other $n_{ph} - 1$ parts composing the first half of the waveform can be reconstructed by taking, step by step, the information from the stator sectors placed $k_{ph}$ positions away from the previous, respectively, in the positive direction of the mechanical angle. This procedure will eventually lead to sector positions that are outside of the simulated portion of the motor, if it features more than one multiplicity. However, this is not an issue since the electromagnetic solution repeats periodically, if the number of poles per multiplicity is even, or anti-periodically, if the number of poles per multiplicity is odd, leading to an inverted waveform polarity in the respective stator sectors. Once this is considered, the letters identifying the various sectors in the sequence can be determined, while for the final assignment of the polarity also the term $k_p$ has to be evaluated. If $k_p$ results an even number, the $k_{ph}$ sector shift will be equivalent to $\theta_{sim}$, so the same polarity is maintained, while if $k_p$ results an odd number the shift will be equivalent to $\theta_{sim} + \theta_p$, which means that the polarity will be inverted at each step since $\theta_p$ corresponds to half of the stator flux density waveform period.

Considering the above, a general procedure to determine the reconstruction sequence is developed and is presented step-by-step in the following example. For the ease of explanation, the example is not made on the reference motor shown in Fig. 1, but for an hypothetical 8 poles, 6 slots DLCW three-phase motor, which, having $k_{ph} = 2$ and $k_p = 3$ both different from 1, represents one of the least trivial cases. The workflow for determining the reconstruction sequence is as follows:

- At first, solve (6) in function of $n_{ph}$ and $2p/m$
$$n_{ph} = 3, \quad p = 4, \quad m = 2, \quad \frac{2p}{m} = 4$$
to retrieve the coefficients $k_{ph}$ and $k_p$.
$$k_{ph} = 2, \quad k_p = 3$$
- Determine the vector composed by the $n_{ph}$ letters identifying the stator sectors in alphabetical order, as
$$[\mathrm{A}, \mathrm{B}, \mathrm{C}]$$
- Concatenate this vector $k_{ph}$ times while maintaining the same polarity if $2p/m$ is even (periodic boundary conditions) or with alternated polarity if $2p/m$ is odd (anti-periodic boundary conditions).
$$[+\mathrm{A}, +\mathrm{B}, +\mathrm{C}, +\mathrm{A}, +\mathrm{B}, +\mathrm{C}]$$

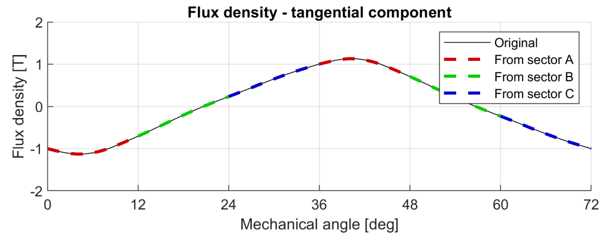

Fig. 3. Reconstructed flux density waveform for the point highlighted in Fig. 2 in phase sector A.

- Select one every $k_{ph}$ terms from the vector, starting from the first, for a total of $n_{ph}$ terms.
$$[+\mathbf{A}, +\mathbf{C}, +\mathbf{B}]$$
- Finally, invert the polarity of the even terms of the sequence if $k_p$ resulted an odd number.
$$[+\mathbf{A}, -\mathbf{C}, +\mathbf{B}]$$

Referring to the 12 slots, 10 poles motor example of Fig. 1, it is instead obtained:
$$n_{ph} = 3, \quad p = 5, \quad m = 2, \quad \frac{2p}{m} = 5$$
$$k_{ph} = 1, \quad k_p = 2$$
Leading to a reconstruction sequence of
$$[+\mathbf{A}, +\mathbf{B}, +\mathbf{C}]$$
While the angle range to be simulated results as
$$\theta_{sim} = \frac{\pi}{p}\frac{1}{n_{ph}} = \frac{\pi}{5}\frac{1}{3} = \frac{\pi}{15}(12^{\circ})$$
An example of the reconstructed flux density waveform for the generic point in sector A, as highlighted in Fig. 2, is finally shown in Fig. 3.

### B. Reconstruction of rotor waveform

The flux density vector in the rotor region is periodical within an angle that corresponds to one stator phase periodicity $\theta_{ph}$, which is equal to the angular extension of one motor multiplicity divided by the number of phases. This occurs because, in a real motor, the flux density as seen from the rotor is not stationary as it would be in the ideal case, which would require an isotropic stator and a perfectly synchronous MMF generated by the stator windings. In an actual motor, the stator anisotropy (always present in slotted, iron-core stators), and the non-synchronous harmonics generated by the stator winding, will create oscillations of the flux density with a period corresponding to $\theta_{ph}$, angle within which both the stator geometry and the MMF generated by the windings will result periodical if seen from the rotor reference frame.

In an analogous way as for the stator, the full flux density waveform in the rotor region, having a periodicity of $\theta_{ph}$, can be actually retrieved by simulating an angle range

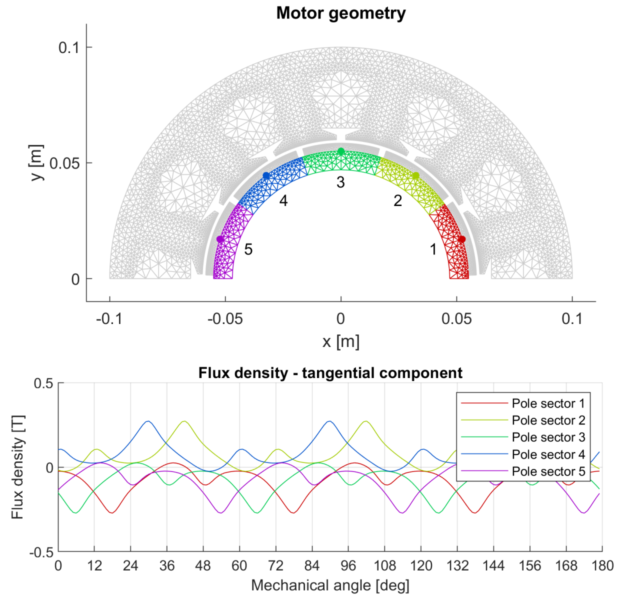


Fig. 4. Example of flux density waveforms in the five pole sectors of the rotor. Waveforms refer to the points highlighted in the top figure. Motor supplied with Iq current only.

corresponding to $\theta_{sim}$, since the angle $\theta_{ph}$ is $2p/m$ times the angle $\theta_{sim}$, and $2p/m$ geometrically symmetrical rotor pole sectors are present within the multiplicity, from which the waveform information can be retrieved with different equivalent phase shifts (see (7)).

$$\theta_{ph} = \frac{2\pi}{m} \cdot \frac{1}{n_{ph}} = \frac{2p}{m} \cdot \frac{\pi}{p} \cdot \frac{1}{n_{ph}} = \frac{2p}{m} \cdot \theta_{sim} \tag{7}$$

More specifically, the flux density waveforms of each of the homologous points found in the $2p/m$ pole sectors are shifted by an angle corresponding to the pole pitch $\theta_p$, and have alternated polarity, as it can be appreciated in Fig. 4. In this case the reconstruction sequence will be defined by a vector containing the $2p/m$ terms identifying the different rotor sectors, with the minus sign used for indicating inverted polarity.

For **integer-slot windings**, the solution is trivial since there is one pole per multiplicity and the flux density waveform results to have the same periodicity as the angle to be simulated, $\theta_{sim}$, meaning that no reconstruction procedure is actually required.

For **fractional-slot windings**, the solution is less trivial and requires the identification of the number of pole sector shifts $k_p$ that leads to an equivalent waveform shift corresponding to $\theta_{sim}$. As similarly done for the stator, the linear Diophantine equation is defined in (8), then resulting in the expression reported in (9), where $k_{ph}$ is the number of times an angle corresponding to $\theta_{ph}$, which is the period of the flux density waveform in the rotor that needs to be subtracted to satisfy the equality.

$$k_p \cdot \theta_p - k_{ph} \cdot \theta_{ph} = \theta_{sim} \tag{8}$$

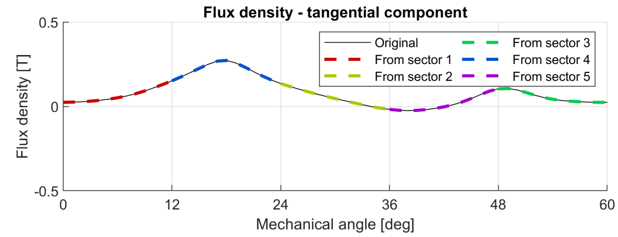


Fig. 5. Reconstructed flux density waveform for the point highlighted in Fig. 4 in pole sector 1.

$$k_p \cdot n_{ph} - k_{ph} \cdot \frac{2p}{m} = 1 \tag{9}$$

It can be observed that equation (9) is equivalent to equation (6) defined for the stator, so the problem has to be solved only once and the same $k_p$ and $k_{ph}$ coefficients can be used to determine the rotor reconstruction sequence. In this case, the variable $k_p$ defines the number of pole sectors steps that lead to an equivalent shift angle of $\theta_{sim}$, while $k_{ph}$ is irrelevant since shifts of an angle corresponding to $\theta_{ph}$ do not change the polarity of the flux density waveform in the rotor, being $\theta_{ph}$ equal to its period.

A procedure for retrieving the reconstruction sequence is proposed, again, aided with the 6 slots, 8 poles motor example.

- Consider $k_{ph}$ and $k_p$ coefficients found solving (6)

$$k_{ph} = 2, \quad k_p = 3$$

- Determine the vector containing the sequence of integer numbers identifying the various pole sectors with alternated polarity, as

$$[+1, -2, +3, -4]$$

- Concatenate this vector $k_p$ times while maintaining the same polarity if $2p/m$ is even (periodic boundary conditions) or with alternated polarity if $2p/m$ is odd (anti-periodic boundary conditions).

$$[+1, -2, +3, -4, +1, -2, +3, -4, +1, -2, +3, -4]$$

- Finally, select one every $k_p$ terms from the vector, starting from the first, for a total of $2p/m$ terms.

$$[\mathbf{+1}, \mathbf{-4}, \mathbf{+3}, \mathbf{-2}]$$

Referring to the 12 slots, 10 poles reference motor of Fig. 1, it is instead obtained:

$$k_{ph} = 1, \quad k_p = 2$$

leading to a reconstruction sequence of

$$[\mathbf{+1}, \mathbf{+3}, \mathbf{+5}, \mathbf{-2}, \mathbf{-4}]$$

An example of the reconstructed rotor flux density waveform for the generic point in sector 1 highlighted in Fig. 4, is finally shown in Fig. 5.

TABLE I

ANGLE RANGE REDUCTION FACTORS AND RECONSTRUCTION SEQUENCES FOR DIFFERENT DLCW MOTOR CONFIGURATIONS

| $N_s/2p$ | $n_{ph}$ | $2p/m$ | $\theta_{Flux}/\theta_{sim}$ | Stator reconstruction sequence | Rotor reconstruction sequence |
|---|---|---|---|---|---|
| 6 / 4 | **3** | 2 | **3** | +A -B +C | +1 -2 |
| 6 / 8 | 3 | **4** | **4** | +A -C +B | +1 -4 +3 -2 |
| 9 / 8 | 3 | **8** | **8** | +A -B +C | +1 -4 +7 -2 +5 -8 +3 -6 |
| 9 / 10 | 3 | **10** | **10** | +A -C +B | +1 -8 +5 -2 +9 -6 +3 -10 +7 -4 |
| 12 / 10 | 3 | **5** | **5** | +A +B +C | +1 +3 +5 -2 -4 |
| 12 / 14 | 3 | **7** | **7** | +A -C -B | +1 -6 -4 -2 +7 +5 +3 |
| 12 / 10 | **6** | 5 | **6** | +A -B +C -D +E -F | +1 -2 +3 -4 +5 |
| 12 / 14 | 6 | **7** | **7** | +A +F -E +D -C +B | +1 +7 -6 +5 -4 +3 -2 |
| 9 / 8 | **9** | 8 | **9** | +A -B +C -D +E -F +G -H +I | +1 -2 +3 -4 +5 -6 +7 -8 |
| 9 / 10 | 9 | **10** | **10** | +A -I +H -G +F -E +D -C +B | +1 -10 +9 -8 +7 -6 +5 -4 +3 -2 |

## V. CASE STUDY: CALCULATION OF IRON LOSSES

The benefit of minimizing the rotor angle range to be simulated is particularly evident in the case of the calculation of iron losses. Since these are derived from the flux density waveforms in the iron regions of the motor, tools included in FE software for their estimation may require a higher angle range to be simulated if a waveform reconstruction technique is not used. For example, in Altair Flux™ the tool included for the calculation of iron losses in post-processing requires to simulate an angle range corresponding to the full period of the flux density waveform in the region where the losses have to be calculated. Only if the the flux density waveform is symmetric, as it happens in the stator region of an electric motor, just half of the period can be simulated enabling an advanced mode feature which reconstructs the waveform antiperiodically [10]. This means that, if losses have to be calculated both in the stator and rotor regions, the required angle range to be simulated is either equal to half of the electrical period, corresponding to the pole pitch $\theta_p$, if $\theta_p > \theta_{ph}$, or equal to the rotor flux density period, corresponding to the phase sector pitch $\theta_{ph}$, if $\theta_{ph} > \theta_p$. Therefore, the angle range reduction factor, defined as the ratio between the angle range required by Flux™, $\theta_{Flux}$, and the minimum one according the waveform reconstruction technique proposed in this paper, $\theta_{sim}$, will be either determined by half of the stator waveform period as in (10), if $\theta_p > \theta_{ph}$, or determined by the rotor waveform period as in (11), if $\theta_{ph} > \theta_p$.

$$\frac{\theta_{Flux}}{\theta_{sim}} = \frac{\theta_p}{\theta_{sim}} = n_{ph} \tag{10}$$

$$\frac{\theta_{Flux}}{\theta_{sim}} = \frac{\theta_{ph}}{\theta_{sim}} = \frac{2p}{m} \tag{11}$$

Examples of the reduction factors that can be achieved are listed in Tab. I for few suitable (i.e. with reasonable winding factor) multi-phase DLCW configurations, along with the corresponding reconstruction sequences for the stator and rotor regions. Being the reduction factor given by the maximum between $n_{ph}$ and $2p/m$, the benefit of the reconstruction procedure is particularly significant for motor configurations with high number of phases and/or high number of poles per multiplicity. The listed reduction factors can be also seen as a theoretical metric to evaluate the reduction in computational load, while the actual reduction in terms of simulation times is not listed as it depends on the software used, the solver settings, and on the actual number of steps simulated itself. In the software used in this analysis for example, Altair Flux™, simulation times tends to increase linearly with respect to the number of steps simulated but with an additional fixed time offset. This means the higher the number of steps computed, the lower the constant time offset is with respect to the overall time, and consequently the closer the simulation speedup will be to the one suggested by the angle range reduction factor. Nevertheless, high angle reduction factor will still lead to significant simulation time reduction even if simulation times do not scale linearly with the number of steps.

## VI. CONCLUSIONS AND POSSIBLE APPLICATIONS

In this paper, a methodology for optimizing the FE analysis procedure of an electric motor has been proposed. The solution allows to retrieve the complete waveform of any variable of the FE electromagnetic solution, e.g. flux density, starting from simulations performed within a reduced rotor angle range, reducing thus the number of steps to be simulated. This is achieved by exploiting additional periodicity conditions of the motor geometry and mesh, as defined in section III. Once those are respected, the motor can be divided into different sections which are subject to the same magnetic conditions, but at a shifted rotor angle. Then, the waveform can be reconstructed from a reduced angle range by properly combining the information retrieved from the different motor sections. Since the order in which the different parts of the waveform have to be combined is not trivial, and is dependent on the specific motor configuration, a generalized procedure for retrieving the correct reconstruction sequence as a function of the motor characteristic has been defined in section IV. Finally, a comparison between the rotor angle span required by a state-of-the-art commercial software for computing iron losses and the one required by the proposed solution is shown. The angle range reduction factor is equal to the maximum between the number of phases and the number of poles per multiplicity. Hence, it is at least three times for all types of three-phase motors and higher for configurations with a greater number of phases and/or poles per multiplicity. In conclusion, the proposed waveform reconstruction procedure has demonstrated significant potential for reducing the computational load of motor analysis, and can find its application into FE motor analysis software. Thanks to its generalization for different motor topologies, its inclusion should be particularly convenient for solutions which already rely on motor templates, which can be easily adapted to satisfy the additional geometrical periodicity conditions required.

## VII. Acknowledgement

This research has received funding from the ”A-IQ Ready” project (grant agreement ID: 101096658) under the European Union’s HORIZON-KDT-JU-2021-2-RIA program.

## References

[1] Altair Flux™ 2022 Documentation, ”Periodicity and periodicity conditions on boundaries” URL: https://2022.help.altair.com/2022/flux/Flux/Help/english/UserGuide/English/topics/PeriodiciteEtConditionsDePeriodiciteSurLesFrontieres.htm?hl=periodicity

[2] JMAG, ”[JFT085] Detailed Rotation Periodic Mesh Settings”, URL: https://www.jmag-international.com/support/mod/tutorial/note/JFT085DetailedPeriodicMesh-e.pdf

[3] B. Zhang, T. Talmon and M. Doppelbauer, “Iron Losses Calculation of a novel Axial flux machine with different Slot-Pole Combinations based on the FEA Results corresponding to one-sixth electrical Period,”th IET International Conference on Power Electronics, Machines and Drives (PEMD 2016), Glasgow, UK, 2016, pp. 1-6, doi: 10.1049/cp.2016.0327.

[4] P. A. Hargreaves, B. C. Mecrow and R. Hall, ”Calculation of Iron Loss in Electrical Generators Using Finite-Element Analysis,” in IEEE Transactions on Industry Applications, vol. 48, no. 5, pp. 1460-1466, Sept.-Oct. 2012, doi: 10.1109/TIA.2012.2209851.

[5] M. M. Billah, F. Martin and A. Belahcen, ”A Computationally Effective Method for Iron Loss Estimation in a Synchronous Machine from a Static Field Solution,” 2020 International Conference on Electrical Machines (ICEM), Gothenburg, Sweden, 2020, pp. 751-757, doi: 10.1109/ICEM49940.2020.9271020.

[6] D. Meeker, ”Rotor Motion using an (Anti)Periodic Air Gap Boundary Condition,” URL: https://www.femm.info/wiki/RotorMotion

[7] D. Meeker, ”Sliding band motion model for electric machines,”, March 2018, doi: 10.13140/RG.2.2.36813.90088.

[8] Marcsa, D. (2017). Rotational Motion Modelling for Numerical Analysis of Electric Machines. Acta Technica Jaurinensis, 10(2), pp. 124–136, doi: 10.14513/actatechjaur.v10.n2.437

[9] K. H. Rosen, ”Primes and Greatest Common Divisors” in *Elementary number theory and its applications*, 6th ed., Boston, MA, USA: Pearson, 2010, pp. 95-109.

[10] Altair Flux™ 2022 Documentation, ”Steps for iron losses computation on regions”, URL: https://2022.help.altair.com/2022/flux/Flux/Help/english/UserGuide/English/topics/EtapesDeCalculDePertesFerSurRegions.htm

## VIII. Biographies

**Alessandro Capitanio** (Student member, IEEE) received the B.S. degree in Vehicle Engineering and the M.S. degree in Advancded Automotive Engineering at the university of Modena and Reggio Emilia, in 2021 and 2023 respectively. He is currently pursuing his Ph.D. degree at the Univerisy of Modena and Reggio Emilia. His main research interests are the design and the control of electrical machines for traction application.

**Giacomo Sala** (Member, IEEE) received the Ph.D. in Electrical Machines and Drives in 2018 from the University of Bologna, Italy. He worked as a researcher until 2019 in the Department of Electrical and Electronic Engineering, The University of Nottingham. Since 2019 he has been working as a researcher at the University of Bologna, Italy, where he is currently employed as an Assistant Professor, since 2020. His research interests include design, modeling and control of multi-phase electrical machines.

**Stefano Nuzzo** (S’17-M’18-SM’23) received his Ph.D. degree in Electrical and Electronic Engineering in 2018 from the University of Nottingham, Nottingham, U.K, where he worked also as a Research Fellow within the Power Electronics, Machines and Control (PEMC) Group. In January 2019, he moved to Modena, Italy, where he is currently a Tenure Track Assistant Professor in Electric Machines and Drives at the Department of Engineering “Enzo Ferrari” of the University of Modena and Reggio Emilia. His research interests are the analysis, modelling and optimization of electrical machines and drives, with focus on sustainability and reliability design approaches of synchronous drives based on radial flux machines for industrial and traction applications. Stefano Nuzzo is currently an Associate Editor for the IEEE PELS Transactions on Transportation Electrification and IEEE PES Transactions on Energy Conversion.

**Gabriele Rizzoli** received the M.Sc. and Ph.D. degrees in electrical engineering from the University of Bologna, Bologna, Italy, in 2012 and 2016, respectively. He is currently an Assistant Professor with the Department of Electrical, Electronic, and Information Engineering “G. Marconi,” University of Bologna. His research interests include the design of electrical machines, the development and control of high-efficient power converters for automotive and renewable energy applications.

**Davide Barater** (Senior Member, IEEE) received the Ph.D. degree in information technology from the University of Parma, Parma, Italy, in 2014. He is currently an Associate Professor at the University of Modena and Reggio Emilia, Modena, Italy. He is the Coordinator of the European Project AUTO-MEA which aims to develop novel solutions for windings structures based on hairpin technology for improved power density, efficiency, and increased frequency operation. https://www.automea.unimore.it. He is the author or co-author of more than 100 papers in scientific journals and international conferences. His research area is focused on power electronics and electrical machines for e-mobility and motor drives. Dr. Barater is the Secretary of the IEEE Industrial Electronics Society Electrical Machines Technical Committee and an Associate Editor of IEEE TRANSACTIONS ON INDUSTRY APPLICATIONS.

**Giovanni Franceschini** received the M.Sc. degree in Electronic Engineering from the University of Bologna, Bologna, Italy. He is currently the Full Professor of Electric Drives with the Department of Engineering “Enzo Ferrari”, University of Modena and Reggio Emilia, Modena, Italy. He was the Coordinator of the European Project ALEA, to achieve complete and accurate lifetime models for electrical drives in aerospace applications. He is the author or co-author of more than 150 international papers. His research interests include power electronics for e-mobility and motor drives control and diagnostic.